

High-Temperature Ferromagnetism in Ni²⁺-Doped ZnO Aggregates Prepared from Colloidal Diluted Magnetic Semiconductor Quantum Dots

Pavle V. Radovanovic and Daniel R. Gamelin

Department of Chemistry, University of Washington, Box 351700, Seattle, Washington 98195-1700, USA

(Received 29 July 2003; published 9 October 2003)

Ferromagnetism with $T_c > 350$ K is observed in the diluted magnetic semiconductor Ni²⁺:ZnO synthesized from solution. Whereas colloidal Ni²⁺:ZnO nanocrystals are paramagnetic, their aggregation gives rise to robust ferromagnetism. The appearance of ferromagnetism is attributed to the increase in domain volumes and the generation of lattice defects upon aggregation. The unusual temperature dependence of the magnetization coercivity is discussed in terms of a temperature-dependent exchange interaction involving paramagnetic Ni²⁺ ions.

DOI: 10.1103/PhysRevLett.91.157202

PACS numbers: 75.50.Dd, 61.72.Vv, 75.50.Pp, 75.50.Tt

Diluted magnetic semiconductors (DMSs) [1] have recently attracted broad interest for their promise in generating and manipulating spin-polarized currents [2]. Optically transparent ferromagnetic DMSs, obtained by doping paramagnetic transition metal ions into wide band gap semiconductors, have received particular attention for integrated optospintronic applications [3,4]. Specifically, ZnO, which has large band gap and exciton binding energies, excellent mechanical characteristics, and is inexpensive and environmentally safe, has been identified as a promising host material. Stable ferromagnetic configurations arising from carrier-mediated exchange interactions have been predicted for several transition-metal-doped ZnO DMSs (TM²⁺:ZnO, TM²⁺ = V²⁺, Cr²⁺, Mn²⁺, Fe²⁺, Co²⁺, Ni²⁺) [5,6]. Room-temperature ferromagnetism has been observed only for V²⁺:ZnO [7], Fe²⁺:ZnO [8], and Co²⁺:ZnO [9,10]. Large variations in magnetic properties have been reported for otherwise similar films, indicating a strong dependence on synthesis and processing conditions. In some cases, even the conclusion of intrinsic ferromagnetism remains controversial. In this Letter, we report high- T_c ferromagnetism in nanocrystalline Ni²⁺:ZnO prepared from solution at low temperatures. High- T_c ferromagnetism has not been reported previously for any Ni²⁺-based DMS, and this discovery narrows the gap between theoretical predictions and experimental results. The appearance of ferromagnetism upon room-temperature aggregation of paramagnetic Ni²⁺:ZnO DMS nanocrystals unambiguously demonstrates its intrinsic origin and additionally represents a significant advance toward chemically controlled spin effects in semiconductor nanostructures.

Preparation of Ni²⁺:ZnO is particularly challenging due to the large driving force for phase segregation into NiO and ZnO [11]. Consequently, relatively few studies of this system have been reported [11–15]. Among these, ferromagnetism has been observed only at 2 K in Ni²⁺:ZnO films (> 3 mol % Ni²⁺) fabricated by pulsed laser deposition using ZnO/NiO ceramic targets [12]. The extremely high analytical Ni²⁺ concentrations (up to

25 mol %), the discontinuous variation in ZnO lattice constant c as a function of Ni²⁺ content, and the striking similarity of the thin film magnetic data to those reported for NiO nanocrystals [16] raise concerns over phase segregation in these films, however.

We have recently reported the synthesis of high-quality colloidal Ni²⁺:ZnO and Co²⁺:ZnO DMS quantum dots (DMS-QDs) [10,13]. This approach provides excellent control over dopant speciation and allows effective isolation and purification of the desired products. Substitutional doping has been demonstrated using ligand-field electronic absorption and magnetic circular dichroism spectroscopies [10,13]. The resulting DMS colloids are highly processable and can be functionalized or assembled into higher-dimensionality structures by bottom-up approaches, offering new opportunities for the study and application of DMSs on the nanometer scale. For this study, a modified synthetic procedure has been used: a suspension of LiOH in EtOH was added to an EtOH solution of Zn(OAc)₂ · 2H₂O and Ni(OAc)₂ · 4H₂O (~ 10 mol % Ni²⁺) at 65 °C. After nucleation, nanocrystals were grown at 25 °C to the desired size. The nanocrystals were selectively precipitated, washed, and resuspended in EtOH to give a clear colloidal dispersion. An isocrystalline core/shell procedure [13,17] involving epitaxial growth of ZnO shell layers on the nanocrystal surfaces was applied to internalize any surface-exposed Ni²⁺. This method is very effective for obtaining internally doped DMS-QDs, but in some cases at the expense of size uniformity. After further purification, the clear colloidal suspensions were concentrated and the nanocrystals were allowed to aggregate slowly over a period of two weeks. The aggregation is irreversible and the nanocrystals cannot be redispersed. Samples were characterized by x-ray diffraction (XRD, CuK_α source) and transmission electron microscopy (TEM, JEOL 2010, and Phillips CM 100). The Ni²⁺ mole fraction was determined using atomic emission spectrometry (Jarrell Ash 955). Electronic absorption spectra were collected at 25 °C using a Cary 5E spectrophotometer. A SQUID

magnetometer (Quantum Design, MPMS-5S) was used for magnetic measurements.

Figure 1(a) shows powder XRD data for slowly aggregated 0.93% \pm 0.05% $\text{Ni}^{2+}:\text{ZnO}$ nanocrystals. The XRD pattern demonstrates highly crystalline wurzite ZnO and is essentially identical to those obtained for freestanding and rapidly aggregated nanocrystals (data not shown). No other crystalline phases have been detected. The XRD linewidths correspond to an average nanocrystal diameter of \sim 6 nm. Figure 1(b) shows a TEM image of the freestanding DMS-QDs from which the aggregates were prepared. A TEM image of the slowly aggregated nanocrystals is shown in Fig. 1(c). The irregularly shaped clusters are several hundreds of nanometers across. The higher-resolution TEM image in Fig. 1(d) reveals a dense network of nanocrystals that largely retain their original size and shape. Although some short-range order may exist, long-range order is clearly absent.

The overview electronic absorption spectrum of the colloidal $\text{Ni}^{2+}:\text{ZnO}$ DMS-QDs is shown in Fig. 2 (solid line). The lowest energy ZnO band gap excitation at ca. $29\,250\text{ cm}^{-1}$ (\sim 3.6 eV) is higher in energy than in bulk (\sim 27 000 cm^{-1} , \sim 3.35 eV [3]) due to quantum confinement. The spin-orbit split ${}^3T_1(F) \rightarrow {}^3T_1(P)$ ligand-field transition of substitutionally doped tetrahedral Ni^{2+} ions is observed at $15\,500\text{ cm}^{-1}$ (solid line, magnified) and matches the corresponding transition in bulk single-crystal $\text{Ni}^{2+}:\text{ZnO}$ (dashed line [14]). Figure 2 also shows the overview absorption spectrum of the aggregates (dotted line). The redshift of the ZnO band gap transition indicates electronic coupling between nanocrystals in the aggregates.

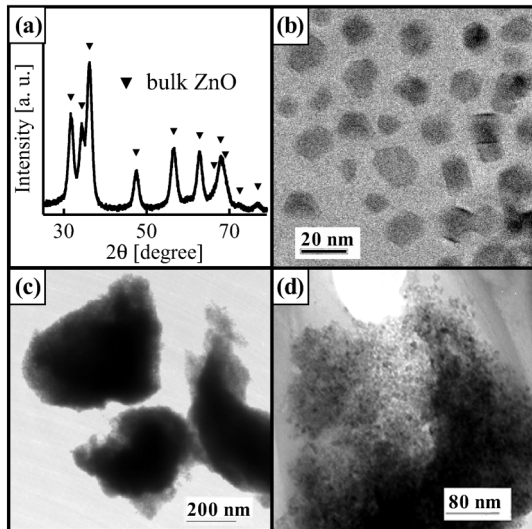


FIG. 1. (a) XRD pattern of 0.93% $\text{Ni}^{2+}:\text{ZnO}$ aggregates prepared by reaction-limited aggregation of colloidal $\text{Ni}^{2+}:\text{ZnO}$ nanocrystals. The bulk ZnO diffraction pattern is indicated (\blacktriangledown). (b) TEM image of freestanding nanocrystals from which the aggregates were prepared. (c) TEM image of the aggregates used for (a). (d) Selected area TEM image of the same aggregates.

157202-2

Figure 3 shows 350 K magnetization data for rapidly and slowly aggregated 0.93% $\text{Ni}^{2+}:\text{ZnO}$ nanocrystals. The rapidly aggregated nanocrystals show little or no long-range magnetic ordering. Similarly, no magnetic ordering could be detected in the freestanding nanocrystals used to form the aggregates. In contrast, a distinct ferromagnetic hysteresis loop is observed for the slowly aggregated nanocrystals. We emphasize that the ferromagnetism in Fig. 3 arises solely from slow room-temperature aggregation of paramagnetic colloidal $\text{Ni}^{2+}:\text{ZnO}$ nanocrystals, with no change in other experimental parameters. The colloidal nanocrystals show no dopant mobility and appear to be stable indefinitely under aggregation conditions, so secondary phases (e.g., NiO or Ni) are unambiguously excluded as the source of the observed ferromagnetism. We therefore conclude that the ferromagnetism in Fig. 3 is an intrinsic property of the true DMS $\text{Ni}^{2+}:\text{ZnO}$. The temperature dependence of the saturation magnetization (M_s) for the hysteresis shows no evidence of a ferromagnetic phase transition (Fig. 3, inset), indicating $T_c > 350\text{ K}$. At 350 K, an average saturation moment of $\sim 0.057\mu_B/\text{Ni}^{2+}$ is determined. This value suggests that only a small fraction of the Ni^{2+} dopants gives rise to all of the observed ferromagnetism. High-field 2 K magnetization measurements verify that the majority of the material is paramagnetic or superparamagnetic. Nevertheless, the high- T_c ferromagnetism shown in Fig. 3 is a fundamentally new phenomenon for Ni^{2+} -based DMSs.

The coercivity (H_c) and percent remanence ($\%M_r/M_s$) at 350 K are 55 Oe and 10%, respectively. Figure 4(a) plots H_c as a function of temperature between 5 and 350 K. H_c increases with temperature up to 100 K and remains constant at higher temperatures. M_r/M_s exhibits the same temperature dependence. Ferromagnetic ordering in ZnO DMSs is suggested to be charge carrier mediated [5,6], in which case a temperature dependence of this type might potentially reflect thermally activated carrier detrapping. This temperature dependence differs from that of analogous ferromagnetic $\text{Co}^{2+}:\text{ZnO}$

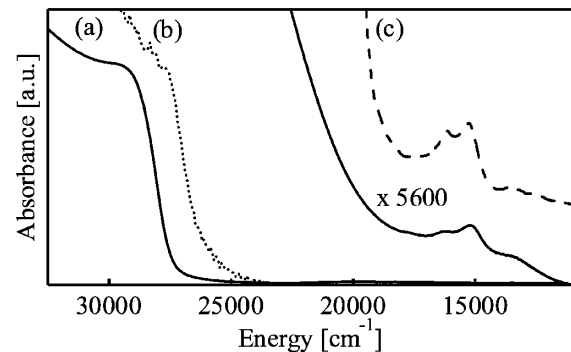


FIG. 2. Absorption spectra of [(a) solid line] colloidal 0.93% $\text{Ni}^{2+}:\text{ZnO}$ DMS-QDs, [(b) dotted line] reaction-limited aggregates formed from the nanocrystals in (a), and [(c) dashed line] bulk 0.1% $\text{Ni}^{2+}:\text{ZnO}$ single crystal [14].

157202-2

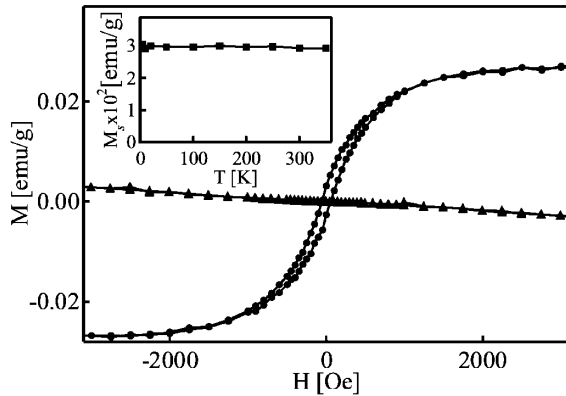


FIG. 3. 350 K M vs H measurements of rapidly (\blacktriangle) and slowly (\bullet) aggregated 0.93% $\text{Ni}^{2+}:\text{ZnO}$ nanocrystals. Inset: Temperature dependence of M_s for the latter.

nanocrystalline aggregates and thin films, however, in which both H_c and M_r/M_s decrease gradually with increasing temperature [10,19]. Furthermore, M_s is temperature independent from 5–350 K (Fig. 3, inset). Only the hysteresis itself shows this temperature dependence. Quantitative analysis of coercivity in these aggregates is complicated by their inhomogeneous fractal structures. Nevertheless, we may associate H_c with an activation barrier, $\Delta\Omega^*$, between local minima in the magnetization potential energy landscape as illustrated in Fig. 4(a) (inset). To reverse the moment of a magnetized sample, the applied field must be sufficient to overcome $\Delta\Omega^*$. The data in Fig. 4(a) therefore indicate that $\Delta\Omega^*$ increases with increasing temperature.

In contrast with the more commonly studied Mn^{2+} and Co^{2+} ions in DMSs, tetrahedral Ni^{2+} possesses both

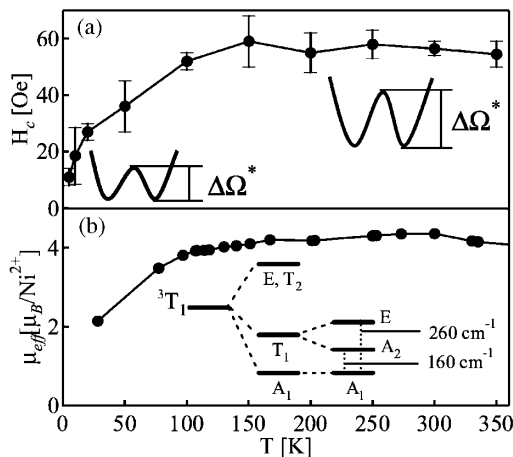


FIG. 4. (a) Temperature dependence of H_c for 0.93% $\text{Ni}^{2+}:\text{ZnO}$ nanocrystalline aggregates. The error bars represent the standard deviation from three measurements. The insets illustrate the change in the barrier to magnetization reversal ($\Delta\Omega^*$) as a function of temperature. (b) Temperature dependence of μ_{eff} for bulk 0.1% $\text{Ni}^{2+}:\text{ZnO}$ [18]. The inset shows the spin-orbit (center) and trigonal (right) splitting pattern of the tetrahedral Ni^{2+} ${}^3T_1(F)$ ground state (left).

orbital and spin angular momentum in its electronic ground state, ${}^3T_1(F)$, giving rise to strong first-order spin-orbit coupling. The ${}^3T_1(F)$ multiplet is further perturbed by the trigonal ligand field provided by wurzite ZnO , resulting in the energy level splitting shown in Fig. 4(b) (inset) [18]. The low-temperature ground state A_1 has no angular momentum ($J = 0$) and is perturbed by a magnetic field only in second order. The first sublevel of a low-symmetry split T_1 state possessing angular momentum ($J = 1$) and a nonzero first-order Zeeman coefficient lies ca. 160 cm^{-1} above the ground state. This electronic structure gives rise to a characteristic temperature dependence of the effective magnetic moment of paramagnetic Ni^{2+} ions [$\mu_{\text{eff}} = 2.828(\chi T)^{1/2}$], in which μ_{eff} increases with increasing temperature below 100 K due to thermal population of the T_1 sublevels. Experimental powder-averaged μ_{eff} data for bulk paramagnetic 0.1% $\text{Ni}^{2+}:\text{ZnO}$ [18] are plotted as a function of temperature in Fig. 4(b). These data bear a remarkable similarity to the temperature dependence in H_c [Fig. 4(a)], from which we conclude that the two must be related. We attribute the temperature dependence of $\Delta\Omega^*$ to temperature-dependent magnetic exchange interactions between the ferromagnetic domains and surrounding paramagnetic Ni^{2+} ions. Such interactions stabilize the magnetized domain against magnetization reversal and therefore increase $\Delta\Omega^*$ [20]. Increasing the temperature increases μ_{eff} of the paramagnetic ions, thereby increasing the exchange energy and, hence, also the coercivity. As a consequence, the same characteristic temperature dependence appears in both μ_{eff} and the hysteresis properties H_c and M_r . The insets of Fig. 4(a) illustrate the change in $\Delta\Omega^*$ from low to high temperatures. In analogously prepared ferromagnetic $\text{Co}^{2+}:\text{ZnO}$ aggregates, μ_{eff} of the paramagnetic Co^{2+} ions is temperature independent above ~ 10 K and the exchange interactions are therefore not evident [10,19].

Finally, we address the remarkable influence of aggregation on the magnetic properties of nanocrystalline $\text{Ni}^{2+}:\text{ZnO}$. Whereas distinct ferromagnetism is observed following slow (reaction-limited) aggregation, it is absent or only weakly observed following rapid (diffusion-limited) aggregation (Fig. 3). Aggregation kinetics have been shown to govern the structural properties of Au, SiO_2 , and other aggregates [21]. The low sticking probabilities that result when interparticle Coulombic repulsion barriers are greater than kT allow aggregating nanocrystals to sample many geometric configurations before binding irreversibly. Consequently, reaction-limited aggregation forms denser aggregates than does diffusion-limited aggregation. The formation of dense aggregates of $\text{Ni}^{2+}:\text{ZnO}$ DMS-QDs under slow aggregation conditions is verified by TEM [Figs. 1(c) and 1(d)] and by the red-shift in the ZnO band gap absorption (Fig. 2).

We propose that the structural differences between $\text{Ni}^{2+}:\text{ZnO}$ DMS-QD aggregates prepared under reaction- and diffusion-limited conditions are directly responsible

for their different magnetic properties. Two factors are considered essential for the conversion of paramagnetic $\text{Ni}^{2+}:\text{ZnO}$ nanocrystals into ferromagnetic DMSs: increased domain volumes and increased carrier concentrations. With average nanocrystal diameters of only ~ 6 nm, domain wall formation within individual nanocrystals is energetically unfavorable and ferromagnetism would be single domain in origin. The activation barrier to magnetization reversal in this limit is the magneto-crystalline anisotropy energy of the domain itself, KV (K is the magneto-crystalline anisotropy coefficient and V is the domain volume). Because of their very small volumes, magnetic reorientation in $\text{Ni}^{2+}:\text{ZnO}$ DMS-QDs should be extremely rapid. Dense aggregation induces strong interparticle electronic coupling that increases V and thus could stabilize ferromagnetism. Interestingly, paramagnetism and not superparamagnetism is observed in the freestanding DMS nanocrystals, indicating that volume changes alone cannot account for the appearance of ferromagnetism upon aggregation and suggesting that the mechanism for long-range magnetic ordering is absent in the freestanding nanocrystals. Carrier doping has been predicted to strongly influence the stability of the ferromagnetic phase in $\text{Ni}^{2+}:\text{ZnO}$, with greater stability predicted for higher n doping [6]. Aggregation likely generates many defects at interfaces between adjacent nanocrystals that are able to induce n -type character [22]. We therefore attribute the appearance of ferromagnetism in nanocrystalline $\text{Ni}^{2+}:\text{ZnO}$ upon reaction-limited aggregation to the combined effects of increased domain volumes and the introduction of n -type lattice defects.

In summary, high- T_c ferromagnetism has been observed in nanocrystalline $\text{Ni}^{2+}:\text{ZnO}$ synthesized from solution. The appearance of ferromagnetism upon aggregation of colloidal paramagnetic $\text{Ni}^{2+}:\text{ZnO}$ nanocrystals is attributed to the increase in domain volumes and the generation of defects at interfaces between nanocrystals. The hysteresis temperature dependence relates to changes in $\Delta\Omega^*$ with temperature that ultimately arise from the spin-orbit ground-state splitting of paramagnetic Ni^{2+} ions exchange coupled to the ferromagnetic domains. These results represent a first step toward the goal of using colloidal DMS nanocrystals as building blocks in the bottom-up assembly of functional magnetic semiconductor nanostructures, and have further exposed the exciting possibility of chemically controlling the magnetic and magnetoelectronic properties of nanoscale DMSs.

Financial support from the NSF (DMR-0239325 and ECS-0224138) is gratefully acknowledged. Acknowledgment is also made to the Research Corporation (RI0832), the ACS-PRF (37502-G), the Semiconductor Research Corporation (2002-RJ-1051G), and the University of Washington (RRF-2651) for partial support of this research, and to the UW Center for Nanotechnology (NSF-IGERT) (P.V.R.). TEM data were collected at EMSL (PNNL), a user facility sponsored by the DOE

and operated by Battelle. Dr. Chongmin Wang (PNNL) is thanked for valuable TEM assistance.

-
- [1] *Diluted Magnetic Semiconductors*, edited by J.K. Furdyna and J. Kossut, Semiconductors and Semimetals Vol. 25 (Academic, New York, 1988).
 - [2] S. A. Wolf, D. D. Awschalom, R. A. Buhrman, J. M. Daughton, S. von Molnár, M. L. Roukes, A. Y. Chthelkanova, and D. M. Treger, *Science* **294**, 1488 (2001); H. Ohno, F. Matsukura, and Y. Ohno, *JSAP Int.* **5**, 4 (2002).
 - [3] S. J. Pearton, C. R. Abernathy, M. E. Overberg, G. T. Thaler, D. P. Norton, N. Theodoropoulou, A. F. Hebard, Y. D. Park, F. Ren, J. Kim, and L. A. Boatner, *J. Appl. Phys.* **93**, 1 (2003).
 - [4] K. Ando, in *Solid-State Sciences: Magneto-Optics* (Springer, New York, 2000), Vol. 128, p. 211.
 - [5] T. Dietl, H. Ohno, F. Matsukura, J. Cibert, and D. Ferriand, *Science* **287**, 1019 (2000).
 - [6] K. Sato and H. Katayama-Yoshida, *Physica (Amsterdam)* **10E**, 251 (2001).
 - [7] H. Saeki, H. Tabata, and T. Kawai, *Solid State Commun.* **120**, 439 (2001).
 - [8] S.-J. Han, J.W. Song, C.-H. Yang, S. H. Park, J.-H. Park, Y. H. Jeong, and K.W. Rhie, *Appl. Phys. Lett.* **81**, 4212 (2002).
 - [9] K. Ueda, H. Tabata, and T. Kawai, *Appl. Phys. Lett.* **79**, 988 (2001); K. Rode, A. Anane, R. Mattana, J.-P. Contour, O. Durand, and R. LeBourgeois, *J. Appl. Phys.* **93**, 7676 (2003).
 - [10] D. A. Schwartz, N. S. Norberg, Q. P. Nguyen, J. M. Parker, and D. R. Gamelin, *J. Am. Chem. Soc.*, <http://dx.doi.org/10.1021/ja036811v>.
 - [11] V. Jayaram and B. S. Rani, *Mater. Sci. Eng. A* **304**, 800 (2001).
 - [12] T. Wakano, N. Fujimura, Y. Morinaga, N. Abe, A. Ashida, and T. Ito, *Physica (Amsterdam)* **10E**, 260 (2001).
 - [13] P.V. Radovanovic, N. S. Norberg, K. E. McNally, and D. R. Gamelin, *J. Am. Chem. Soc.* **124**, 15 192 (2002).
 - [14] H. A. Weakliem, *J. Chem. Phys.* **36**, 2117 (1962).
 - [15] K. Ando, *cond-mat/0208010*.
 - [16] N. Cordente, B. Toustou, V. Colliere, C. Amiens, B. Chaudret, M. Verelst, M. Respaud, and J.-M. Broto, *C.R. Acad. Sci. Paris, Chem.* **4**, 143 (2001); F. Bødker, M. F. Hansen, C. Bender Koch, and S. Mørup, *J. Magn. Magn. Mater.* **221**, 32 (2000).
 - [17] P.V. Radovanovic and D. R. Gamelin, *J. Am. Chem. Soc.* **123**, 12207 (2001).
 - [18] W. H. Brumage and C. C. Lin, *Phys. Rev.* **134**, A950 (1964).
 - [19] P.V. Radovanovic and D. R. Gamelin (to be published).
 - [20] V. Skumryev, S. Stoyanov, Y. Zhang, G. Hadjipanayis, D. Givord, and J. Nogués, *Nature (London)* **423**, 850 (2003).
 - [21] D. A. Weitz, J. S. Huang, M. Y. Lin, and J. Sung, *Phys. Rev. Lett.* **54**, 1416 (1985).
 - [22] S. B. Zhang, S.-H. Wei, and A. Zunger, *Phys. Rev. B* **63**, 075205 (2001).